ACS chemical biology

Articles

pubs.acs.org/acschemicalbiology

Structure−Activity Relationships Reveal Key Features of 8-Oxoguanine: A Mismatch Detection by the MutY Glycosylase

Amelia H. Manlove,[†] Paige L. McKibbin,[†] Emily L. Doyle,[†] Chandrima Majumdar,[†] Michelle L. Hamm,[‡] and Sheila S. David*[,†]

[†]Department of Chemistry, University of California at Davis, One Shields Avenue, Davis, California 95616, United States

[‡]Department of Chemistry, University of Richmond, Richmond, Virginia 23173, United States

Supporting Information

ABSTRACT: Base excision repair glycosylases locate and remove damaged bases in DNA with remarkable specificity. The MutY glycosylases, unusual for their excision of undamaged adenines mispaired to the oxidized base 8-oxoguanine (OG), must recognize both bases of the mispair in order to prevent promutagenic activity. Moreover, MutY must effectively find OG:A mismatches within the context of highly abundant and structurally similar T:A base pairs. Very little is known about the factors that initiate MutY's interaction with the substrate when it first encounters an intrahelical OG:A mispair, or about the order of recognition checkpoints. Here, we used structure−activity relationships (SAR) to investigate the features that influence the *in vitro* measured parameters of mismatch affinity and adenine base excision efficiency by *E. coli* MutY. We also evaluated the impacts of the same substrate alterations on MutY-mediated repair in a cellular context. Our results show that MutY relies strongly on the presence of the OG base and recognizes multiple structural features at different stages of recognition and catalysis to ensure that only inappropriately mispaired adenines are excised. Notably, some OG modifications resulted in more dramatic reductions in cellular repair than in the *in vitro* kinetic parameters, indicating their importance for initial recognition events needed to locate the mismatch within DNA. Indeed, the initial encounter of MutY with its target base pair may rely on specific interactions with the 2-amino group of OG in the major groove, a feature that distinguishes OG:A from T:A base pairs. These results furthermore suggest that inefficient substrate location in human MutY homologue variants may prove predictive for the early onset colorectal cancer phenotype known as MUTYH-Associated Polyposis, or MAP.

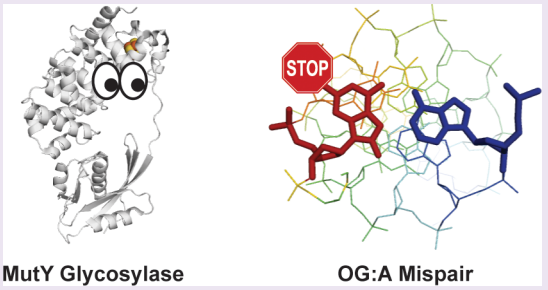

Routine oxidative damage due to cellular processes is known to include the common guanine oxidation product 8-oxo-7,8-dihydroguanine (OG).[1,2] With only two more atoms than canonical guanines, the OG lesion can be interpreted by polymerases correctly as a G, or incorrectly as a T (Figure 1A). In response to this dual coding effect, cells have evolved a context-dependent base excision repair (BER) system to address the OG lesion, known as the "GO repair pathway" (Figure 1B).[3−5] The *E. coli* DNA glycosylase Fpg is responsible for removing the OG lesion when paired opposite C, while MutY removes miscoding adenines opposite the lesion. In this pathway, MutY and its homologues provide a "failsafe" mechanism for OG glycosylases like Fpg, acting as a final barrier to irreparable mutations caused by OG. The importance of MutY's activity is demonstrated by near-universal homologue conservation from prokaryotes to eukaryotes, and by its disease-relevance in humans as exemplified by an inherited colorectal cancer syndrome known as MUTYH-associated polyposis, or MAP.[2,5−7]

MutY displays many commonalities with other glycosylases and DNA-binding proteins, along with important differences that set it apart. Along with a growing number of glycosylases, MutY contains a $[4Fe{-}4S]^{2+}$ cofactor that is required for activity.[7−11] MutY enzymes are also distinct from other BER glycosylases in possessing a unique C-terminal domain (CTD) that is highly homologous to the NUDIX d(OG)TP hydrolase NUDT1; moreover, the CTD has been shown to be crucial for OG recognition and repair.[12,13] Structural insights into the lesion recognition process have been provided by several crystal structures using either a cleavage-resistant 2′-deoxy-2′-fluoroadenosine analog, an inactive enzyme, or a transition state mimic to capture a glimpse of MutY on the cusp of catalysis.[15−17] At the late stage visualized in these structures, the OG:A bp has been disrupted, and the adenine has been extruded from the helix and placed into an extrahelical pocket where catalysis occurs (Figure 2).[2,17−19] A Tyr residue is inserted between OG and its 5′ neighbor, suggesting a role in disrupting the OG:A bp and stabilizing the severe kink in the DNA.[15−17,20] Notably, the CTD makes contact with the OG lesion, which has shifted in conformation from OG_{syn} when paired to A, to OG_{anti} when MutY-bound.[13,15,16] Such dramatic changes in DNA conformation (Figure 2) could potentially

Received: May 10, 2017
Accepted: July 19, 2017
Published: July 19, 2017

DOI: 10.1021/acschembio.7b00389
ACS Chem. Biol. 2017, 12, 2335−2344

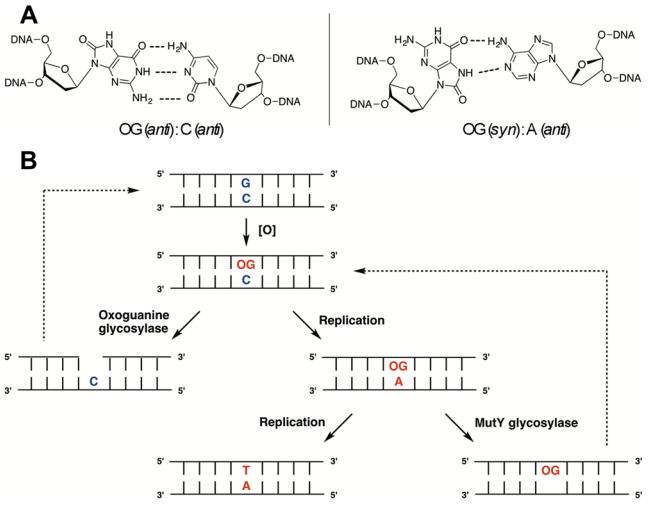

Figure 1. Pairing behavior and repair of OG. (A) OG is found paired to both C and A in DNA. (B) Repair of OG lesions is mediated *via* the GO Repair Pathway.

provide multiple checkpoints for the enzyme to achieve its remarkable substrate specificity. MutY, like many DNA binding proteins, is known to utilize a processive search mechanism along DNA;[21] however it is currently unknown how MutY effectively locates and discriminates OG:A pairs from other A-containing pairs such as T:A or G:A during this search process. The task required of MutY is daunting when considering the rarity of OG:A pairs compared to T:A pairs in a cellular context.

In this work, we aimed to use structure−activity relationships to help elucidate the interactions of MutY with the OG substrate base. We have used a range of experimental techniques to examine specific aspects of MutY's reaction, from substrate binding, to catalysis, to participation in cellular repair. Glycosylase assays, under single- or multiple-turnover conditions, were used to isolate the rates of catalysis and product release, respectively. Gel shift assays with a binding-competent but catalytically inactive mutated enzyme were employed to determine binding efficiency. A bacterial cell-based assay allowed us to contrast *in vitro* enzyme behavior with the efficiency of MutY-mediated repair under the more demanding conditions of living cells. By using analogs of the OG base in all of these experiments, we have correlated structural features of OG with their effects on binding, catalysis, product release, and overall repair efficiency in *E. coli* cells. Our results indicate that the identity of the OG lesion is confirmed by multiple interactions on both the Watson−Crick and Hoogsteen faces of the OG base. Additionally, the results herein support the idea that MutY relies on the presence of the OG lesion first to efficiently select miscoding adenines and then to help catalyze the remote cleavage of the adenine base from DNA. Most strikingly, our results suggest that the initial recognition of an OG:A mispair may occur through a single interaction of MutY with the intrahelical OG base.

RESULTS AND DISCUSSION

Choice of Oxoguanine Analogs to Investigate Substrate Recognition Requirements. A series of purine and deazapurine nucleotides (Figure 3) were chosen that represent relatively minor changes to the OG base on either the pyrimidine or the imidazole ring. These analogs were incorporated into oligomeric DNA and paired opposite an adenine base in the complementary strand to mimic MutY's natural OG:A substrate. The choice of specific analog bases was informed by a number of structural and biochemical studies of MutY and other DNA glycosylases.[15,16,22−25] In the majority of cases, appropriate analogs were not commercially available; thus the choice of analogs was also informed by practical considerations such as synthetic feasibility and potential structural instability.

Analogs of OG were included that display reduced Watson−Crick complementarity to cytosine (1MOG, 8OA); these analogs were expected to retain the ability to base pair with A but would be expected to interfere with late-stage OG recognition contacts that are observed in MutY-lesion crystal structures (Figure 2D).[15−17] Whereas 1-methyl-8-oxo-7,8-dihydroguanine (1MOG) provides a simple steric block to pairing at one location on the Watson−Crick face, 8-oxo-7,8-dihydroadenine (8OA) retains only the imidazole ring features of OG and instead presents the Watson−Crick binding face of

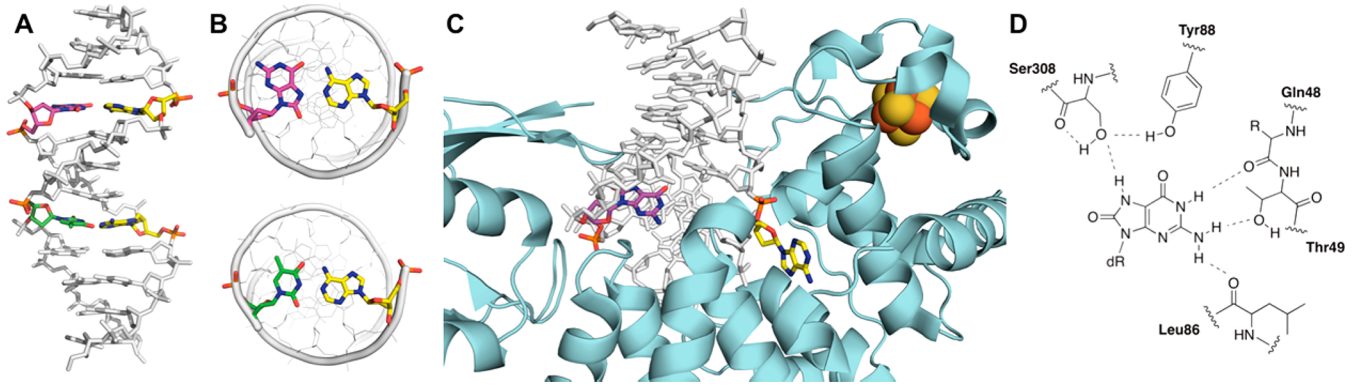

Figure 2. Dramatic conformational changes between unbound and MutY-bound, catalytically ready substrate DNA. (A) Side views of substrate OG (purple) paired to A (yellow) and nonsubstrate T (green):A (yellow) pairs illustrate the lack of major helix deformation by the presence of an OG:A pair (PDB entry 178D). (B) Cutaway views of OG:A (top) and T:A (bottom) base pairs show the major and minor groove faces that MutY must discriminate.[14] (C) In the catalytic complex of *Geobacillus stearothermophilus* MutY with OG and a noncleavable A analog, the DNA helix is bent, and the backbone around the scissile adenine is sharply kinked to place the adenine base in the active site pocket (PDB entry 3G0Q). (D) Strictly conserved contacts between MutY residues and the OG base as observed in crystal structures.[15−17] Note the absence of a direct H-bond to the 8-oxo group of OG. Residue numbers correspond to the *G. stearothermophilus* protein.

DOI: 10.1021/acschembio.7b00389
ACS Chem. Biol. 2017, 12, 2335−2344

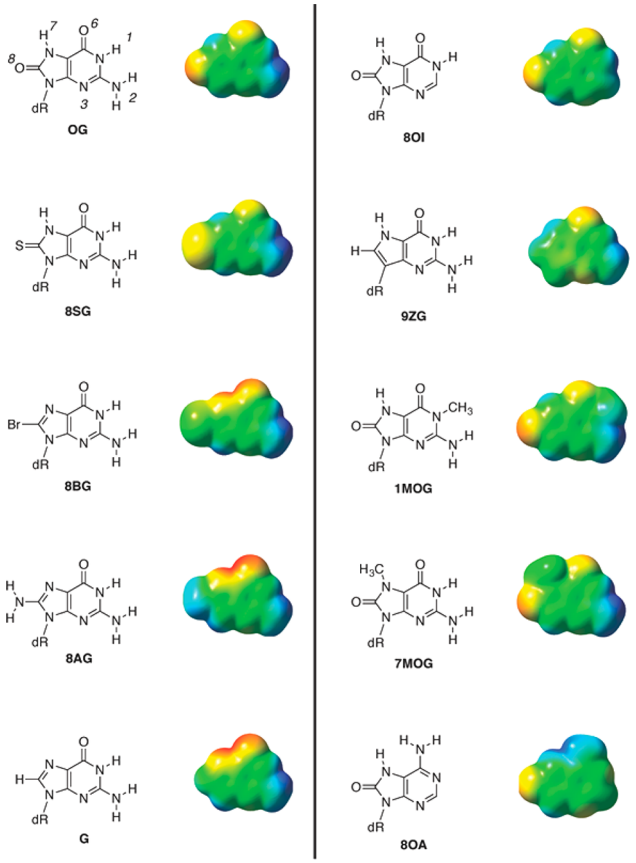

Figure 3. Analogs of OG used in this study and their electrostatic potential surfaces. For visual clarity and simplicity, only the free nucleobase of each analog was used for electrostatic potential modeling.

an adenine.[26] Notably, 8OA:A pairs are substantially more destabilized than OG:A pairs, comparable to an A:A or C:A mismatch, and MutY has been observed to have weak activity toward adenines in this pairing context.[24,26]

To investigate the impact of altering the Hoogsteen face of OG, we incorporated changes that would alter H-bonding to A or disfavor the *syn* conformation (G, 9ZG, 8AG, 8BG, 7MOG, 8OA). Each of these analogs could increase the rate of base flipping by locally destabilizing the region near the introduced base pair; however, disfavoring *syn* pairing with A may also alter the proper groove placement of base pair recognition elements within duplex DNA. In addition, altering the NH7 donor of OG would also be anticipated to alter late-stage H-bonding interactions observed in the MutY-lesion structures (Figure 2). 7-Methyl-8-oxo-7,8-dihydroguanine (7MOG) sterically impedes pairing to A with a methyl group that blocks effective hydrogen bonding, while 8-aminoguanine (8AG) and 8-bromoguanine (8BG) lack a hydrogen bond donor at N7.[27,28] 8OA preserves the Hoogsteen face but replaces a hydrogen bond acceptor with a donor at the 6-position of the purine.[26] Both G and 9-deazaguanine (9ZG) lack the 8-substituent that drives the shift from predominantly *anti* to predominantly *syn* conformation.[29] However, 9ZG:A pairs are more stable to thermal denaturation than G:A mismatches because 9ZG retains a hydrogen bond donor at N7 that can help stabilize the Hoogsteen pairing to A.[30]

Two analogs were also included to act as relatively close mimics of OG in terms of base pairing and coding during DNA replication. 8-Thioguanine (8SG) displays an increase in the bulk of the 8-substituent along with a mild decrease in that substituent's electronegativity; this analog shows similar conformational and base pairing proclivities to OG.[30] The base of 8-oxoinosine (8OI) lacks the exocyclic amine of OG, producing a Watson–Crick face that typically codes like G under experimental conditions.[31] Likewise, duplexes containing 8SG:A and 8OI:A pairs have similar duplex stabilities to those harboring OG:A pairs.[30]

Rates of Adenine Cleavage (k_2). We evaluated the ability of wild type *E. coli* MutY to excise adenine opposite the chosen analogs using a PAGE-based glycosylase assay with a radiolabeled 30 base pair substrate duplex. Under single turnover conditions ([E] > [DNA]), substrate binding is rapid, and the observed rate of product formation corresponds to the rate of catalysis, k_2 (Scheme 1). Briefly, the A-containing strand was 5′-

Scheme 1. Minimal Kinetic Scheme for the Reaction of *E. coli* MutY with OG:A Pairs

$$\text{MutY + (DNA)}_S \underset{}{\overset{K_d}{\rightleftharpoons}} \text{MutY(DNA)}_S \xrightarrow{k_2} \text{MutY(DNA)}_P \xrightarrow{k_3} \text{MutY + (DNA)}_P$$

radiolabeled and annealed to a complement strand to produce Duplex 1 with a central target X:A base pair, where X is OG or an analog (Figure 4A). At defined time points, sodium hydroxide was used to quench the enzymatic reaction and cleave the abasic site product to provide a 14-nucleotide product fragment. The substrate and product oligonucleotides (denoted in Figure 4B as DNA_S and DNA_P, respectively) were separated by denaturing polyacrylamide gels and quantitated following storage phosphor autoradiography. The production curves were fitted to the appropriate rate equation.[25]

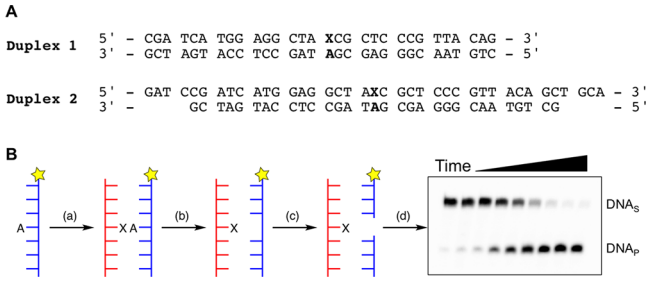

Figure 4. DNA duplexes and experimental determination of glycosylase activity. (A) Duplexes used in this work. (B) Schematic representation of the glycosylase assay for kinetic characterization of MutY's enzymatic behavior with substrate analog pairs. The radiolabeled A-containing strand is (a) annealed to an analog-containing complement, (b) treated with MutY, (c) quenched with NaOH to cleave the resulting abasic site product, and (d) the resulting DNA fragments are visualized with denaturing PAGE and storage autoradiography.

Whereas MutY cleaves adenine from OG:A pairs at a rate of 12 ± 1 min^{-1}, the enzyme displayed widely variable ability to cleave adenines opposite the analogs studied (Figure 5A). Observed glycosylase rates (Table 1) ranged from little or no decrease in k_2, as with 8SG:A (10 ± 3 min^{-1}) pairs and 8OI:A (6 ± 1 min^{-1}), to extremely poor cleavage, as with 1MOG:A pairs (0.014 ± 0.003 min^{-1}). Notably, MutY was able to achieve complete conversion of the substrate to product with most of the analog-containing duplexes under these conditions; only the slowest reactions (1MOG:A, 8AG:A, and 9ZG:A)

DOI: 10.1021/acschembio.7b00389
ACS Chem. Biol. 2017, 12, 2335–2344

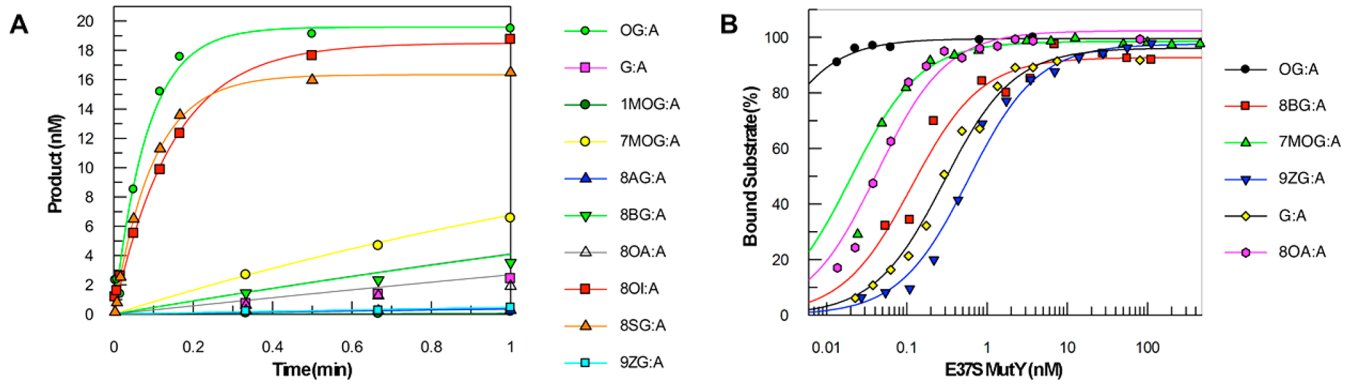

Figure 5. *In vitro* product accumulation and binding curves. (A) Representative fits of adenine cleavage from X:A pairs by MutY under single turnover conditions. Differences in final amplitude (cf. 8SG:A vs OG:A) were determined to be due to experiment-to-experiment variation. For X:A pairs with the smallest k_2 values, the exponential fit overestimates the maximum rate (cf. 8BG:A), and therefore a linear fit, using only the early time points for these samples, was used to obtain a more accurate value for k_2. (B) Representative fits of binding curves from enzyme titration experiments with E37S MutY. For clarity, some analogs with very similar binding constants to the shown data were omitted (OG:A and 8SG:A; 9ZG:A and 8AG:A; G:A and 1MOG:A; 8OA:A and 8OI:A; see Table 1 for values). Duplexes containing OG:A and 8SG:A pairs were bound at all enzyme concentrations tested.

Table 1. Substrate Dissociation Constants, Catalytic Rates and Product Release Rates of MutY DNA Glycosylase with Various OG Analogs Paired to A

base pair	K_d (pM)	k_2 (min^{-1})	k_3 (min^{-1})
OG:A	<3[a]	12 ± 1[b]	0.003 ± 0.001
8SG:A	<3[a]	10 ± 3	0.004 ± 0.004
8OI:A	40 ± 10	6 ± 1	0.003 ± 0.002
7MOG:A	20 ± 10	0.6 ± 0.1	0.004 ± 0.001
G:A	240 ± 80	0.28 ± 0.06	NB[c]
8BG:A	110 ± 40	0.21 ± 0.06	NB
8OA:A	40 ± 20	0.13 ± 0.05	0.02 ± 0.01
9ZG:A	600 ± 400	0.031 ± 0.008	NB
8AG:A	500 ± 200	0.016 ± 0.003	NB
1MOG:A	300 ± 200	0.014 ± 0.003	NB

[a]An upper limit of the K_d is estimated based on the DNA concentration used in the experiments. [b]The error reported is the standard deviation from a minimum of three trials. [c]NB: no burst phase detected under multiple turnover conditions.

were unable to reach completion in hour-long experiments. Sulfur is a competent mimic of O^8 in 8SG:A pairs in terms of MutY-catalyzed excision, while other 8-substituents resulted in reduced activity. The presence of an 8-substituent that favors the *syn* conformation is not enough to support high activity as indicated by the reduced k_2 values for 8BG:A and 8AG:A (60- and 750-fold) substrates. Notably, the 8BG:A and G:A pairs are similarly processed, further underscoring the importance of an oxo-like functional group at this position. A feature of the 8-oxo group in OG is that it demands the presence of an NH at N7, and this facilitates the favorable pairing to A. Our results indicate that the presence of an NH at this position alone is insufficient to support efficient catalysis; indeed, 9ZG:A pairs were among the least efficiently processed. In addition, blocking the N-7 position with a methyl group but retaining the 8-oxo-substituent in 7MOG:A substrates resulted in only a 20-fold reduced efficiency of adenine excision, underscoring the influence of the 8-oxo group on MutY-catalyzed excision.

Surprisingly, the individual change that had the most dramatic impacts on adenine cleavage resulted from capping N1 with a methyl group (1MOG:A, 0.014 ± 0.003 min^{-1}). The change at N1 was more deleterious than removal of O^8 that is considered the hallmark of OG. The poor activity of MutY on 1MOG:A substrates may result not only from the loss of N1H but from the methyl group preventing proper engagement in the OG binding site. 8OA:A pairs also lack an exchangeable proton at N1 but were somewhat better substrates for MutY (0.13 ± 0.05 min^{-1}). This may be due to favorable effects of the presence of the 8-oxo-substituent, in conjunction with the ability of the N^6 hydrogen bond donor of 8OA to replace a lost interaction between OG's N1−H and the backbone oxygen of Gln42 in the final stages of catalysis (homologous to *G. stearothermophilus* Gln48 in Figure 2D). Interestingly, the effects at different positions are not isolated nor directly correlated. For instance, G lacks both O^8 and H^7, yet adenine was cleaved faster from G:A pairs than from those containing 9ZG, which lacks only O^8 but shows severely compromised cleavage (0.031 ± 0.008 min^{-1}).

Rates of Abasic Site Product Release (k_3). When the glycosylase assay (Figure 4B) is performed under multiple turnover conditions with the natural substrate, MutY is strongly inhibited by its apurinic (AP) site product.[25] The half-life of the complex between MutY and an OG:AP-containing duplex is greater than 3 h, which is observed experimentally as an initial "burst" of product followed by an extremely slow steady-state rate. This biochemical behavior allows the separation of the chemistry rate from the product release rate by simple changes in relative concentrations of enzyme and substrate. We therefore investigated whether each X:A pair displayed a slower steady-state rate of product formation following the initial burst of AP site formation, similar to OG:A pairs. Only 8SG, 8OI, and 7MOG displayed product release rates that were similar to the native substrate (Table 1). With 8OA:A substrates, the burst is subtle, but defined enough to determine a product release rate of 0.02 ± 0.01 min^{-1}, indicating the importance of both the Watson−Crick and Hoogsteen face of OG for high affinity for the product. The other analogs lacked a detectable burst phase due to their relatively slow catalytic rates, similar to G:A pairs.[1,25] Notably, the presence of an 8-oxo-like substituent impacts both efficient adenine excision (k_2), as well as the high affinity for the product leading to a small product release rate k_3.

Substrate Binding Prior to Catalysis. Because the chemistry step of adenine cleavage is relatively fast and MutY

DOI: 10.1021/acschembio.7b00389
ACS Chem. Biol. 2017, 12, 2335−2344

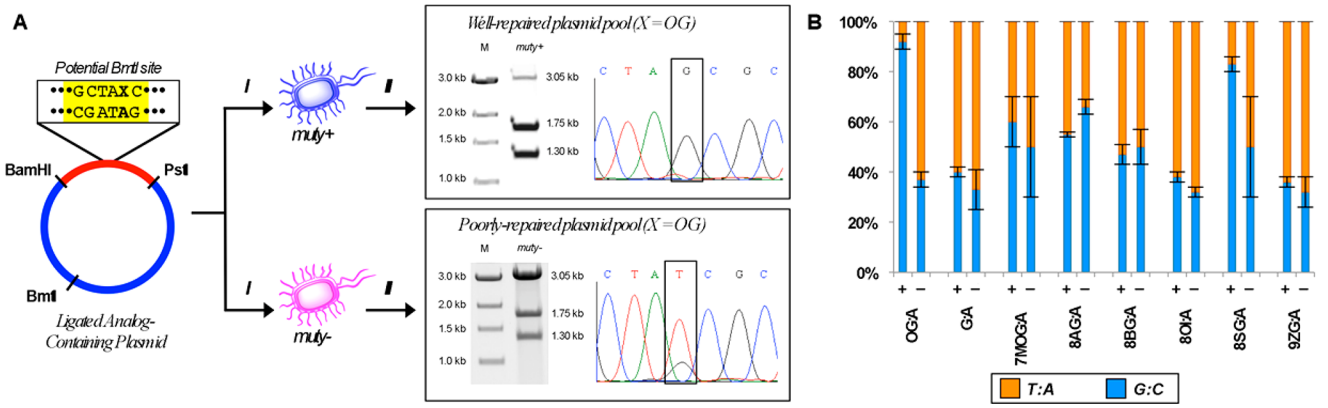

Figure 6. Determining the cellular repair of OG analogs. (A) *E. coli* cell-based assay of MutY-mediated repair. Substrate plasmids containing a single, site-specific X:A pair (X = OG or an analog thereof) are prepared by ligating a sticky-ended duplex containing the X:A pair into an unmethylated linear piece of the pACYC177 plasmid.[1] The substrate plasmid is transformed into *muty*+ and *muty*− cell lines to observe their repair capacity. The pool of plasmids that is isolated following repair and replication displays a distribution of base pairs at the location of the original X:A pair. G:C pairs at this location produce a second BmtI restriction site that can be observed using gel electrophoresis as two bands with 1.30 kb and 1.75 kb lengths; other base pairs that may result at this location (typically T:A) result in a single 3.05 kb band following BmtI digestion. Sequencing is also used to provide a more direct visualization of the types of base pairs that result at the location of the original X:A pair. (B) Percentage of resulting G:C and T:A base pairs at the site of the original X:A pair in an *E. coli* cell-based assay in the presence (+) or absence (−) of wild type MutY. G:C content was determined by digestion with *Bam*HI.[1] 8OA and 1MOG in the original substrate plasmid resulted in no discernible amount of G:C pairs. Sequencing traces of these samples showed that 100% T:A pairs resulted in place of an original 1MOG:A pair, and a roughly equal distribution of T:A and A:T pairs resulted in place of 8OA:A. Error bars represent the standard deviation from the mean.

binds tightly to abasic sites, standard electrophoretic mobility shift assays (EMSA) with radiolabeled DNA and wild-type MutY result in a measurement that reflects a mixture of enzyme−substrate and enzyme−product complexes. A convenient strategy for evaluating relative substrate affinity by MutY involves stalling catalysis by using either a cleavage-resistant substrate or a catalytically inactive mutated MutY. Although cleavage-resistant 2′-deoxyadenosine analogs can be used for this purpose, we felt that the use of analogs in place of both nucleotides in the substrate pair would complicate our analyses. We chose instead to use catalytically inactive E37S MutY that has been well characterized by our laboratory.[1,32] In E37S MutY, the glutamic acid residue that initiates glycosidic bond cleavage by protonating the scissile adenine at N7 has been replaced with serine; notably, this enzyme form retains high affinity and differential binding for specific and nonspecific DNA, similar to the wild type protein. Importantly, we observed complete binding of all of the analog duplexes with the inactive variant.

Of the analogs tested, only 8SG:A pairs (Table 1) were bound with similar affinity to OG:A pairs (below the ∼3 pM limit of detection). The remaining analogs ranged in affinity, with equilibrium dissociation constants ranging from 20 pM to 600 pM (Figure 5). The presence of the 8-oxo-group correlates with the next highest affinity group of substrate analogs, 8OI:A, 7MOG:A, and 8OA:A, which all exhibit an approximately 10-fold reduced binding affinity (K_d's of 20−40 pM) by MutY compared to OG:A. The influence of the oxo-group for high affinity binding is not readily explained with the MutY-lesion structures since there are no direct contacts to the 8-oxo group (Figure 2D). In contrast, the measured decreases in affinity with these three 8-oxo-containing analogs correlate with the loss of late-stage OG interactions observed in the MutY-lesion structures. The high affinity for analogs retaining the 8-oxo group suggests that it plays an important role in "locking" MutY into a high affinity conformation on the lesion mispair. The remaining analogs exhibit further reduced binding (another ∼10-fold) ranging from 100−600 pM in the following order of K_d: 8BG:A < G:A < 1MOG:A < 8AG:A < 9ZG:A. Notably, 1MOG retains the 8-oxo group yet is much more reduced in affinity relative to the other 8-oxo-containing analogs. This additional erosion in affinity suggests that the methyl group at N1 may prevent full engagement in the OG-binding site, as well as remove an important H-bonding contact in the MutY−lesion complex. Thus, these results point to the importance of both the Watson−Crick face and Hoogsteen face of OG for the exceptionally high affinity of MutY for its native substrate and suggest a recognition checkpoint which involves simultaneous recognition of both faces of OG.

Recognition and Repair in Living Bacterial Cells. MutY-mediated repair in a cellular setting was observed by transforming *muty*+ or *muty*− cell lines with a plasmid containing a single site-specific X:A pair that was created by ligation of a sticky-ended X:A-containing duplex (Duplex 2) into a plasmid fragment derived from pACYC177 (Figure 6A). Transformed populations of each cell line were allowed to grow and to replicate the substrate plasmid.[1] The amplified plasmid pools from at least five transformations were isolated and analyzed by restriction digestion and sequencing to determine the distribution of base pairs that resulted at the lesion location (Figure 6B). In these assays, OG:A-containing plasmids are fully repaired to the correct G:C base pairs in the presence of MutY (routinely ∼95%); G:A base pairs, while substrates for MutY *in vitro*, are not repaired significantly over the background. In the absence of MutY, the background levels of G:C and T:A base pairs that result at the location of an OG:A mispair (∼35% G:C, ∼65% T:A) reflect replication across both bases of the mispair, with the OG coding partially like T to result in less than 50% final G:C content.[1] The coding properties of the substrate analogs are also reflected in the distribution of base pairs that are observed in the plasmids that are retrieved from the *muty*− cells (Figure 6). For instance, 8OA is nonmutagenic and codes like adenine;[33] hence, the resulting mixture of roughly 1:1 A:T and T:A pairs observed in

DOI: 10.1021/acschembio.7b00389
ACS Chem. Biol. 2017, 12, 2335−2344

the sequencing traces reflects the unrepaired replication of both strands. 8SG was the only analog that displayed any amount of MutY-mediated repair, as evidenced by a change in the observed base pair distribution of *muty+* and *muty−* cells; adenines opposite 8SG were repaired by MutY with a small but statistically significant ($P < 0.02$) decrease in efficiency compared to adenines opposite OG. For all other analogs, the types and percentages of base pairs observed at the original analog base pair site were the same whether the plasmids were retrieved from *muty+* or *muty−* cell lines (Figure 6B), indicating no MutY-mediated repair for adenines opposite 8AG, 8BG, 8OA, 8OI, 9ZG, 1MOG, or 7MOG.

Correlation of Catalysis and Substrate Binding Affinity. In general, the analogs that retain high affinity for MutY also are processed the most efficiently (Figure 7). This is

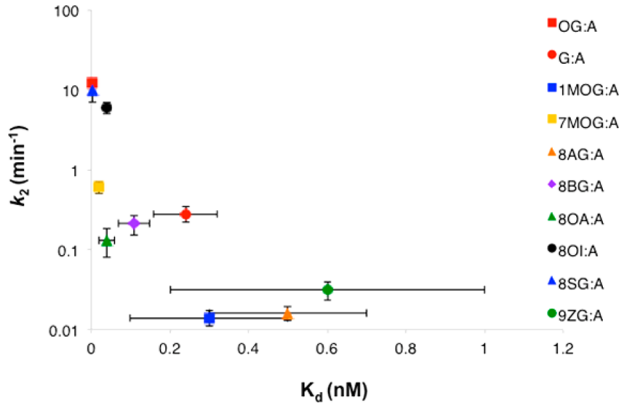

Figure 7. Rate of adenine cleavage (k_2) by MutY versus substrate binding affinity (K_d) for X:A substrate pairs, where X is an analog of the OG base. Note the log scale of the *y* axis, which obscures the vertical error bars in cases such as OG:A pairs. Error bars represent the standard deviation from the mean.

not completely unexpected insofar as enzymatic catalysis cannot occur in the absence of enzyme−substrate binding. Notable exceptions to the correlation between high affinity and efficient excision were observed. For instance, although MutY had similar substrate affinity for 8OI:A pairs compared to 7MOG:A and 8OA:A pairs, 8OI:A pairs were catalyzed 10-fold more efficiently than 7MOG:A pairs and 40-fold more efficiently than 8OA:A pairs. Likewise, the substrate affinity of MutY to 8AG:A, 8BG:A, 1MOG:A, 9ZG:A, and G:A pairs were all within error of each other, but catalytic rates with these substrates varied substantially, with the fastest reactions (with G:A substrates) catalyzed 20-fold faster than the slowest (1MOG:A pairs). Rates of adenine removal from G:A, 8BG:A, and 8OA:A pairs were within error of one another; however, MutY exhibited a much greater affinity for the 8OA:A substrate. Notably, MutY cleaved adenines from G:A mismatches more readily than all analog pairs but 7MOG, 8OI, and 8SG-containing pairs, which suggests that neither the strength of *syn* conformational preference nor retention of a G-like Watson−Crick face or a OG-like Hoogsteen face are absolutely required for substrate processing. In the case of G:A, the lack of the 8-oxo substituent may impede initial recognition and base pair disruption; however, the similar Watson−Crick faces of G and OG may permit proper engagement in the OG-binding pocket needed to support adenine cleavage, albeit at a reduced rate compared to OG:A bps.

A feature that arises from this comparison of affinity and catalysis is that MutY may be exhibiting *unproductive* binding with some of the analog pairs and that, effectively, not all binding events are equal in leading to and promoting catalysis. Furthermore, these results indicate that the OG base has long-distance effects on the engagement of the scissile adenine into the extrahelical pocket, confirming that OG recognition takes precedence and occurs prior to recognition of the cleaved base to prevent cleavage of adenines from inappropriate pairing contexts. For example, MutY affinity for G:A and 1MOG:A bps are similar, but the adenine glycosylase is considerably slower with 1MOG:A suggesting that the absence of the proper G-like NH donor in 1MOG alters the ability to optimally place the adenine for excision. Similarly, MutY binds 8OA:A pairs 6-fold more tightly than G:A bps but excises adenine 2-fold slower from 8OA:A pairs, again pointing to long-range communication between the OG binding site and adenine excision site. Furthermore, comparing binding and catalysis indicates that some defects in binding do not dramatically alter catalysis. This is most striking with 8OI:A where MutY affinity is reduced at least 10-fold compared to OG:A, but base excision catalysis is only reduced 2-fold, further illustrating that all binding interactions do not impinge equally on the *in vitro* kinetic parameters for catalysis.

Correlation of Catalysis with Product Release. Catalysis and product release are inherently related insofar as they are only distinct when $k_2 \gg k_3$. This was observed in the lack of a burst of product formation for those substrate analogs that displayed slower catalysis by MutY: G, 1MOG, 8AG, 8BG, 8OA, and 9ZG (Table 1). Only three analog-containing base pairs retained a burst of product formation: 7MOG:A, 8OI:A, and 8SG:A. Importantly, the extremely tight product binding displayed by MutY and other glycosylases is thought to be a mechanism for regulating the inherently cytotoxic AP-site product; from these data, it is clear that the presence of OG is the determining factor in the exceptionally tight product regulation of MutY rather than the presence of the AP site itself. Furthermore, there appeared to be no change that would alter the product release term without altering the efficiency of base excision, indicating very tight coupling of the presence of the OG base to the preceding catalytic steps. These results underscore the importance of an oxo-like functionality in the nonscissile base for high affinity for the *substrate and product*, and concomitantly efficient *in vitro* adenine excision, and slow-AP site product release.

Correlation of Cellular Repair with *in Vitro* Enzymatic Behavior. Despite the wide range of observed catalytic rates and binding affinities of the substrate analogs tested, we were surprised to find that we did not observe a similar broad spectrum in the levels of observed cellular repair. The most conservative analog, 8SG, displayed a mild reduction in cellular repair in spite of showing no statistically significant difference in substrate binding, catalysis, or product release *in vitro*. This result suggests that even very subtle changes may have reverberating effects on the broader scale of cellular repair and underscores the idea that MutY exhibits tight control over opposite base recognition. Indeed, for 8SG to impact cellular repair in the face of retained kinetic behavior suggests that this control is extreme and includes factors as yet beyond our experimental reckoning.

All the other analogs eluded MutY completely in the cellular setting. Notably, this includes 8OI:A pairs, which showed a total ablation of MutY-mediated repair in cells despite being

DOI: 10.1021/acschembio.7b00389
ACS Chem. Biol. 2017, 12, 2335−2344

similar in catalytic rate to the repairable 8SG:A pairs. We attribute this startling loss of repair to an inability to effectively locate and intercept the 8OI:A in the cellular context. The potential origin of the defect leading to the absence of repair is hinted at by the 10-fold decrease in affinity observed in the EMSA experiment with E37S MutY and the 8OI:A-containing duplex. Catalytic efficiency would be expected to be a combination of catalysis and binding affinity (related to a specificity factor k_2/K_d); however, in previous work we showed that large decreases in k_2 do not result in significant levels of reduced cellular repair as long as OG:A-like affinity for the mismatch is retained. Specifically, we observed that OG:Z3 (Z3 = 3-deazaadenine) pairs are repaired in cells as efficiently as OG:A pairs despite a 200-fold reduction in k_2.[1] This correlation was also illustrated by analysis of specific mutations in catalytic residues in MutY that did not alter OG:A affinity.[19] In comparison to the WT enzyme, the mutated enzymes in that work displayed much larger decreases in k_2/K_d (200 to 300-fold) than the decrease in k_2/K_d observed here between OG and 8OI (25-fold), and yet, unlike the complete elimination of cellular repair observed with the WT enzyme and 8OI:A pairs, those mutated enzymes retained a significant ability to mediate the repair of OG:A mispairs. The lack of a direct correlation with k_2/K_d underscores that measured defects in k_2 and K_d do not equally impact cellular repair. We suggest the differential impacts are due to magnifying binding defects in a cellular context. Indeed, location and engagement of substrate base pairs would be expected to be more difficult in a cellular context than on a 30-bp duplex *in vitro* due to the much higher concentration of highly similar normal T:A bps compared to OG:A mismatches. In addition, competition for DNA with other cellular proteins may also magnify the consequences of small differences in DNA affinity.[34]

The 2-Amino Group of OG Is a Key Intrahelical Recognition Feature. In comparing OG:A to T:A pairs, the presence of the 2-amino group in the major groove stands out as the major structural difference (Figure 1). We were initially surprised that the removal of the 2-amino group of OG in 8OI:A substrates resulted in only minor changes in *in vitro* glycosylase activity; however, considering the *in vitro* results alongside the absence of cellular repair implicates the 2-amino group recognition as a key element of early stages of detection of OG:A bps. Notably, an important role of the 8-oxo group of OG is favoring the *syn* conformation, and allowing for stable base pairing with A. Moreover, the OG_{syn}:A_{anti} base pairing conformation presents the 2-amino group of OG on the *major groove* side of the DNA helix. In prevalent G:C bps, the 2-amino group of G is localized in the minor groove. Thus, the presence of the 2-amino group in the major groove distinguishes OG:A bps from both T:A and G:C bps. Interestingly, recent structural work by Verdine and co-workers provided a glimpse of MutY interacting with an intrahelical OG:A bp by utilizing disulfide cross-linking with a mutant of the N-terminal domain of MutY that was incapable of extruding adenine.[35] In this structure, the helix−hairpin−helix motif of the N-terminal domain is loosely engaged with the DNA phosphodiester backbone from the minor groove side, and the DNA is its canonical B-form. Comparing this structure to that of full-length MutY bound to lesion-containing DNA suggested that a loop region of the C-terminal domain may be in proximity to interact with OG:A from the major groove side.[35] Due to the known role of the CTD in OG recognition,[13,20,34,36−38] and its required presence for cellular repair of OG:A mismatches,[20,39] the idea that this CTD loop region could be important for OG_{syn} recognition *via* interactions with the 2-amino group is appealing. Indeed, these recognition features could involve direct hydrogen-bonding or steric interactions that aid in stalling MutY as it moves along DNA. Studies to address such ideas are presently in progress.

Lesion Verification Occurs *via* Multiple Checkpoints. The SAR revealed herein, taken together with previous structural and biochemical studies of MutY and related enzymes, provides insight into the key features of the OG:A mismatch that facilitate its efficient and selective recognition and repair by MutY. In the initial processive search process, we suggest that the projection of the 2-amino group of the OG_{syn}:A_{anti} mismatch provides the steric blockade that results in MutY pausing at the target bp. At this intrahelical recognition stage, the 8-oxo functional group likely participates in detection by MutY only indirectly. By creating a new hydrogen bond donor at N7, the oxo functional group facilitates a favorable OG_{syn} base pair with A and thereby forces the 2-amino group of OG to jut into the major groove. Once paused, MutY may also make additional contacts with the 2-amino group and further probe the OG:A bp by inducing a DNA bend at the lesion site. Bending and insertion of the MutY Tyr probe residue (Tyr88 in *G. stearothermophilus* MutY, see Figure 2D) from the minor groove facilitates OG:A base pair opening. The preferential disruption of OG:A bps may also be facilitated by steric clashes specific to the 8-oxo group that ensue as a result of the base pair buckling induced by the probe ligand insertion and DNA bending in a manner conceptually analogous to that used by Fpg in recognition of OG:C bps.[40] Once the bp has been disrupted, the OG is placed within the OG pocket in the *anti* conformation, and the A is effectively inserted into the catalytic active site for cleavage. Full engagement of the OG within the OG site requires extensive interactions with multiple functional groups on both the Watson and Crick and Hoogsteen face of OG, but not directly with the 8-oxo group. The proper positioning of OG at this final stage prior to catalysis is communicated *via* proper "locking" of MutY and potentially *via* a hydrogen-bond network to the A cleavage site that positions catalytic residues appropriately for adenine excision. Only proper orientation of OG at this final stage, tightly clamped at both the Watson−Crick and Hoogsteen faces, allows for efficient adenine excision providing the final substrate verification.

Using this multistep confirmation process, MutY exerts strong opposite base control and avoids mutagenic action on adenines opposite other bases; by linking the binding of OG to catalysis at the distant adenine, the protein effectively uses OG as an activator for catalysis. Importantly, this insight suggests that at least part of the OG binding process overlaps temporally with adenine cleavage and thus is not entirely separable from catalysis.

Lesion Verification Process and MAP. The importance of key aspects of the "OG" revealed in the SAR highlight the structural motifs and specific amino acids of MutY that are involved in mediating interactions with the OG at various stages during the repair process. The critical role of the 2′-amino of OG revealed herein provides additional insight into the importance of the C-terminal domain and the region that is critical for this initial contact. There are over 100 MAP-associated missense variants that are localized throughout MUTYH, with many localizing to the C-terminal domain and other regions that are likely to interact with the OG lesion.[5]

DOI: 10.1021/acschembio.7b00389
ACS Chem. Biol. 2017, 12, 2335−2344

Indeed, one of the most common MAP variants, Y165C, corresponds to the Tyr probe residue that intercalates 5′ to OG and plays an important role in the activity of MutY and MUTYH.[6,20,34,37,39,41] In many cases, however, it is not obvious based on available structural and functional data why some variants would be dysfunctional and associated with MAP. Based on the high impact of modifications of OG described here, mutations that alter recognition and binding to OG would be expected to be particularly detrimental. Moreover, our work indicates that *in vitro* analysis alone may not accurately represent the dysfunction of variants that are involved in initial recognition and lesion detection. These results further underscore the importance of fully understanding the features required for efficient repair to predict the potential impact and disease risk of a given MAP variant.

METHODS

General Methods and Materials. Commercially available enzymes were purchased from New England Biolabs and used according to the manufacturer's protocol. [γ-^{32}P]-ATP was purchased from PerkinElmer. Storage phosphor autoradiographs were scanned on a GE Healthcare Typhoon Trio phosphorimager. Quantitation and data analysis were performed using ImageQuant TL v5.2 (GE Healthcare Life Sciences), GraFit v5.0.2 (Erithacus Software), and Excel v14.7.3 (Microsoft). Electrostatic potential maps were produced using Gaussian09d (Gaussian, Inc.). Aqueous solutions were prepared using distilled, deionized water from a Milli-Q PF purification system. All other reagents were purchased from Sigma-Aldrich, ThermoFisher Scientific, Qiagen, or VWR.

DNA Substrate Preparation. For OG and the 8AG, 8BG, 8OA, and 9ZG analogs, precursor nucleoside amidites suitable for solid phase DNA synthesis were purchased from Glen Research. For 8SG, 7MOG, and 8OI, nucleoside amidites were synthesized as previously reported.[42−46] In the case of 1MOG, the nucleoside amidite was synthesized with substantial modifications from the literature (see Supporting Information). OG-containing and analog-containing DNA oligonucleotides were synthesized at the University of Utah core facility. DNA oligonucleotides containing only standard nucleobases were purchased from Integrated DNA Technologies. All DNA oligonucleotides were purified by HPLC on a Beckman Gold Nouveau system using a Dionex 100 ion exchange column. Deprotection of 8SG-containing oligonucleotides was performed as previously reported after HPLC purification.[43] Masses of the single-stranded substrate oligonucleotides were confirmed by ESI-MS. A representative ESI-MS of a 1MOG-containing oligonucleotide is shown in the Supporting Information. Complementary oligonucleotide sequences were annealed overnight in annealing buffer (20 mM Tris-HCl, 10 mM EDTA, and 150 mM NaCl). Duplex 1 (Figure 4A) was used for all glycosylase and binding assays. Duplex 2 was used for ligation into the substrate plasmid for the cellular repair assay.

MutY Purification, Glycosylase, and Binding Assays. Wild type MutY and E37S MutY were overexpressed, purified on a GE Healthcare AKTA FPLC system, and quantitated as previously described.[1,47] The fraction of binding-competent E37S MutY was determined by binding titrations of the enzyme with an OG:A substrate (20 nM). All enzyme concentrations were corrected for percent activity. Glycosylase assays to measure k_2 and k_3, as well as substrate binding assays to measure apparent K_d were performed as previously described.[25,48] For reactions too fast to measure manually, a KinTek RQF-3 Rapid-Quench instrument was used.

Cellular Repair Assay. Measurements of MutY-initiated base excision repair were performed as previously described[1] using a variety of substrate plasmids. Briefly, substrate plasmids were created by ligating Duplex 2 into a stretch of linear DNA from vector pACYC177 to produce pACYC(OG:A), pACYC(8BG:A), pACYC(8AG:A), pACYC(8SG:A), pACYC(G:A), pACYC(9ZG:A), pACYC-(7MOG:A), pACYC(1MOG:A), pACYC(8OA:A), and pACYC-(8OI:A). Each plasmid was transformed into *muty*+ or *muty*− bacterial cell lines, then amplified and isolated by midiprep (Promega Wizard). BmtI restriction analysis in conjunction with agarose gel electrophoresis gave percent repair to G:C pairs specifically; sequencing was used to confirm the restriction analyses and to identify other base pairs (i.e., T:A and A:T) that resulted at the initial lesion site.

ASSOCIATED CONTENT

Supporting Information

The Supporting Information is available free of charge on the ACS Publications website at DOI: 10.1021/acschembio.7b00389.

Synthesis and characterization of 1MOG-containing nucleotide and oligonucleotides (PDF)

AUTHOR INFORMATION

Corresponding Author

*E-mail: ssdavid@ucdavis.edu.

ORCID

Sheila S. David: 0000-0001-5873-7935

Author Contributions

A.H.M., P.L.M., M.L.H., and S.S.D. designed the study. M.L.H. synthesized the 8SG and 7MeOG phosphoramidites. A.H.M. synthesized 1MOG- and 8OI-containing phosphoramidites. The purifications of DNA, enzyme, and cellular assays were performed by A.H.M., P.L.M., E.L.D., and C.M. A.H.M. and S.S.D. wrote the paper with input from the other authors.

Notes

The authors declare no competing financial interest.

ACKNOWLEDGMENTS

The work was supported by grants from the National Institutes of Health CA067985 (S.S.D.) and NSF 1305548 (M.L.H.). A.H.M was a predoctoral trainee supported by T32-GM008799 from NIGMS-NIH. A.H.M. was also supported by the UCD Department of Chemistry and by GAANN and Corson-Dow Fellowships. M.L.H. is a Henry Dreyfus Teacher Scholar. The authors gratefully acknowledge the assistance of B. Hudson in creating the electrostatic potential maps in Gaussian. The contents are solely the responsibility of the authors and do not necessarily represent the official views of the NIGMS or National Institutes of Health.

ABBREVIATIONS

AP, apurinic; BER, base excision repair; bp, base pair; CTD, C-terminal domain; EDTA, ethylene diamine tetraacetate; EMSA, electrophoretic mobility shift assay; ESI-MS, electrospray ionization mass spectrometry; FPLC, fast protein liquid chromatography; HPLC, high-performance liquid chromatography; MAP, MUTYH-associated polyposis; OG, 8-oxoguanine; PAGE, polyacrylamide gel electrophoresis; SAR, structure−activity relationship; Z3, 3-deazaadenine; 1MOG, 1-methyl-8-oxoguanine; 7MOG, 7-methyl-8-oxoguanine; 8AG, 8-aminoguanine; 8BG, 8-bromoguanine; 8OA, 8-oxoadenine; 8OI, 8-oxoinosine; 8SG, 8-thioguanine; 9ZG, 9-deazaguanine

REFERENCES

(1) Livingston, A., O'Shea, V., Kim, T., Kool, E., and David, S. (2008) Unnatural substrates reveal the importance of 8-oxoguanine for in vivo mismatch repair by MutY. *Nat. Chem. Biol. 4*, 51−58.

(2) David, S., O'Shea, V., and Kundu, S. (2007) Base-excision repair of oxidative DNA damage. *Nature 447*, 941−950.

DOI: 10.1021/acschembio.7b00389
ACS Chem. Biol. 2017, 12, 2335−2344

(3) Slupska, M., Baikalov, C., Luther, W., Chiang, J., Wei, Y., and Miller, J. (1996) Cloning and sequencing a human homolog (hMYH) of the Escherichia coli mutY gene whose function is required for the repair of oxidative DNA damage. *J. Bacteriol. 178*, 3885−3892.
(4) David, S., and Williams, S. D. (1998) Chemistry of glycosylases and endonucleases involved in base-excision repair. *Chem. Rev. 98*, 1221−1262.
(5) Manlove, A., Nuñez, N., and David, S. (2017) The GO Repair Pathway: OGG1 and MUTYH, in *The Base Excision Repair Pathway* (Wilson, D. M., III, Ed.), 1st ed., pp 63−115, World Scientific Press, Singapore.
(6) Al-Tassan, N., Chmiel, N., Maynard, J., Fleming, N., Livingston, A., Williams, G., Hodges, A., Davies, D., David, S., Sampson, J., and Cheadle, J. (2002) Inherited variants of MYH associated with somatic G: C -> T: A mutations in colorectal tumors. *Nat. Genet. 30*, 227−232.
(7) Banda, D., Nuñez, N., Burnside, M., Bradshaw, K., and David, S. (2017) Repair of 8-oxoG:A mismatches by the MUTYH glycosylase: Mechanism, metals and medicine. *Free Radical Biol. Med. 107*, 202.
(8) Cunningham, R., Asahara, H., Bank, J., Scholes, C., Salerno, J., Surerus, K., Munck, E., McCracken, J., Peisach, J., and Emptage, M. (1989) Endonuclease III is an iron-sulfur protein. *Biochemistry 28*, 4450−4455.
(9) Hinks, J., Evans, M., De Miguel, Y., Sartori, A., Jiricny, J., and Pearl, L. (2002) An iron-sulfur cluster in the family 4 uracil-DNA glycosylases. *J. Biol. Chem. 277*, 16936−16940.
(10) Michaels, M., Pham, L., Nghiem, Y., Cruz, C., and Miller, J. (1990) MutY, an adenine glycosylase active on G-A mispairs, has homology to endonuclease III. *Nucleic Acids Res. 18*, 3841−3845.
(11) Lukianova, O., and David, S. (2005) A role for iron-sulfur clusters in DNA repair. *Curr. Opin. Chem. Biol. 9*, 145−151.
(12) Noll, D., Gogos, A., Granek, J., and Clarke, N. (1999) The C-Terminal Domain of the Adenine-DNA Glycosylase MutY Confers Specificity for 8-Oxoguanine·Adenine Mispairs and May Have Evolved from MutT, an 8-Oxo-dGTPase. *Biochemistry 38*, 6374−6379.
(13) Chmiel, N., Golinelli, M., Francis, A., and David, S. (2001) Efficient recognition of substrates and substrate analogs by the adenine glycosylase MutY requires the C-terminal domain. *Nucleic Acids Res. 29*, 553−564.
(14) McAuley-Hecht, K., Leonard, G., Gibson, N., Thomson, J., Watson, W., Hunter, W., and Brown, T. (1994) Crystal Structure of a DNA Duplex Containing 8-Hydroxydeoxyguanine-Adenine Base Pairs. *Biochemistry 33*, 10266−10270.
(15) Lee, S., and Verdine, G. (2009) Atomic substitution reveals the structural basis for substrate adenine recognition and removal by adenine DNA glycosylase. *Proc. Natl. Acad. Sci. U. S. A. 106*, 18497−18502.
(16) Fromme, J., Banerjee, A., Huang, S., and Verdine, G. (2004) Structural basis for removal of adenine mispaired with 8-oxoguanine by MutY adenine DNA glycosylase. *Nat. Mater. 427*, 652−656.
(17) Woods, R., O'Shea, V., Chu, A., Cao, S., Richards, J., Horvath, M., and David, S. (2016) Structure and stereochemistry of the base excision repair glycosylase MutY reveal a mechanism similar to retaining glycosidases. *Nucleic Acids Res. 44*, 801−810.
(18) Michelson, A., Rozenberg, A., Tian, Y., Sun, X., Davis, J., Francis, A., O'Shea, V., Halasyam, M., Manlove, A., David, S., and Lee, J. (2012) Gas-Phase Studies of Substrates for the DNA Mismatch Repair Enzyme MutY. *J. Am. Chem. Soc. 134*, 19839−19850.
(19) Brinkmeyer, M., Pope, M., and David, S. (2012) Catalytic Contributions of Key Residues in the Adenine Glycosylase MutY Revealed by pH-dependent Kinetics and Cellular Repair Assays. *Chem. Biol. 19*, 276−286.
(20) Livingston, A., Kundu, S., Henderson Pozzi, M., Anderson, D., and David, S. (2005) Insight into the roles of tyrosine 82 and glycine 253 in the Escherichia coli adenine glycosylase MutY. *Biochemistry 44*, 14179−14190.
(21) Francis, A., and David, S. (2003) Escherichia coli MutY and Fpg utilize a processive mechanism for target location. *Biochemistry 42*, 801−810.
(22) Bulychev, N., Varaprasad, C., Dormán, G., Miller, J., Eisenberg, M., Grollman, A., and Johnson, F. (1996) Substrate Specificity of Escherichia coli MutY Protein. *Biochemistry 35*, 13147−13156.
(23) Lu, A.-L., Tsai-Wu, J.-J., and Cillo, J. (1995) DNA Determinants and Substrate Specificities of Escherichia coli MutY. *J. Biol. Chem. 270*, 23582−23588.
(24) Michaels, M., Tchou, J., Grollman, A., and Miller, J. (1992) A repair system for 8-oxo-7,8-dihydrodeoxyguanine. *Biochemistry 31*, 10964−10968.
(25) Porello, S., Leyes, A., and David, S. (1998) Single-turnover and pre-steady-state kinetics of the reaction of the adenine glycosylase MutY with mismatch-containing DNA substrates. *Biochemistry 37*, 14756−14764.
(26) Kim, S., Kim, J., Baek, A., and Moon, B. (2002) Base pairing properties of 8-oxo-7,8-dihydroadenosine in cDNA synthesis by reverse transcriptases. *Bioorg. Med. Chem. Lett. 12*, 1977−1980.
(27) Venkatarangan, L., Sivaprasad, A., Johnson, F., and Basu, A. (2001) Site-specifically located 8-amino-2′-deoxyguanosine: thermodynamic stability and mutagenic properties in Escherichia coli. *Nucleic Acids Res. 29*, 1458−1463.
(28) Hamm, M., Rajguru, S., Downs, A., and Cholera, R. (2005) Base Pair Stability of 8-Chloro- and 8-Iodo-2′-deoxyguanosine Opposite 2′-Deoxycytidine: Implications Regarding the Bioactivity of 8-Oxo-2'-deoxyguanosine. *J. Am. Chem. Soc. 127*, 12220−12221.
(29) Cheng, X., Kelso, C., Hornak, V., de los Santos, C., Grollman, A., and Simmerling, C. (2005) Dynamic behavior of DNA base pairs containing 8-oxoguanine. *J. Am. Chem. Soc. 127*, 13906−13918.
(30) Hamm, M., Crowley, K., Ghio, M., Del Giorno, L., Gustafson, M., Kindler, K., Ligon, C., Lindell, M., McFadden, E., Siekavizza-Robles, C., and Summers, M. (2011) Importance of the C2, N7, and C8 Positions to the Mutagenic Potential of 8-Oxo-2′-deoxyguanosine with Two A Family Polymerases. *Biochemistry 50*, 10713−10723.
(31) Yasui, M., Suenaga, E., Koyama, N., Masutani, C., Hanaoka, F., Gruz, P., Shibutani, S., Nohmi, T., Hayashi, M., and Honma, M. (2008) Miscoding Properties of 2′-Deoxyinosine, a Nitric Oxide-Derived DNA Adduct, during Translesion Synthesis Catalyzed by Human DNA Polymerases. *J. Mol. Biol. 377*, 1015−1023.
(32) Francis, A., Helquist, S., Kool, E., and David, S. (2003) Probing the requirements for recognition and catalysis in fpg and MutY with nonpolar adenine isosteres. *J. Am. Chem. Soc. 125*, 16235−16242.
(33) Wood, M., Esteve, A., Morningstar, M., Kuziemko, G., and Essigmann, J. (1992) Genetic effects of oxidative DNA damage: comparative mutagenesis of 7,8-dihydro-8-oxoguanine and 7,8-dihydro-8-oxoadenine in Escherichia coli. *Nucleic Acids Res. 20*, 6023−6032.
(34) Pope, M., Chmiel, N., and David, S. (2005) Insight into the functional consequences of hMYH variants associated with colorectal cancer: distinct differences in the adenine glycosylase activity and the response to AP endonucleases of Y150C and G365D murine MYH. *DNA Repair 4*, 315−325.
(35) Wang, L., Chakravarthy, S., and Verdine, G. (2017) Structural Basis for the Lesion-scanning Mechanism of the Bacterial MutY DNA Glycosylase. *J. Biol. Chem. 292*, 5007−5017.
(36) Kundu, S., Brinkmeyer, M., Eigenheer, R., and David, S. (2010) Ser 524 is a phosphorylation site in MUTYH and Ser 524 mutations alter 8-oxoguanine (OG): A mismatch recognition. *DNA Repair 9*, 1026−1037.
(37) Chmiel, N., Livingston, A., and David, S. (2003) Insight into the functional consequences of inherited variants of the hMYH adenine glycosylase associated with colorectal cancer: Complementation assays with hMYH variants, and pre-steady-state kinetics of the corresponding mutated E-coli enzymes. *J. Mol. Biol. 327*, 431−443.
(38) Pope, M., Porello, S., and David, S. (2002) Escherichia coli apurinic-apyrimidinic endonucleases enhance the turnover of the adenine glycosylase MutY with G: A substrates. *J. Biol. Chem. 277*, 22605−22615.
(39) Kundu, S., Brinkmeyer, M., Livingston, A., and David, S. (2009) Adenine removal activity and bacterial complementation with the human MutY homologue (MUTYH) and Y165C, G382D, P391L and

DOI: 10.1021/acschembio.7b00389
ACS Chem. Biol. 2017, 12, 2335−2344

Q324R variants associated with colorectal cancer. *DNA Repair 8*, 1400−1410.
(40) Qi, Y., Spong, M., Nam, K., Banerjee, A., Jiralerspong, S., Karplus, M., and Verdine, G. (2009) Encounter and extrusion of an intrahelical lesion by a DNA repair enzyme. *Nature 462*, 762−766.
(41) Raetz, A., Xie, Y., Kundu, S., Brinkmeyer, M., Chang, C., and David, S. (2012) Cancer-associated variants and a common polymorphism of MUTYH exhibit reduced repair of oxidative DNA damage using a GFP-based assay in mammalian cells. *Carcinogenesis 33*, 2301−2309.
(42) Hamm, M., and Billig, K. (2006) Oligonucleotide Incorporation and Base Pair Stability of 7-Methyl-8-oxo-2′-deoxyguanosine. *Org. Biomol. Chem. 4*, 4068−4070.
(43) Hamm, M., Cholera, R., Hoey, C., and Gill, T. (2004) Oligonucleotide incorporation of 8-thio-2′-deoxyguanosine. *Org. Lett. 6*, 3817−3820.
(44) Kim, H., Lee, K., Park, B., Ryu, D., Kim, K., Lee, C., Park, S., Han, J., Lee, H., Lee, H., and Han, G. (2006) Synthesis, enzymatic inhibition, and cancer cell growth inhibition of novel delta-lactam-based histone deacetylase (HDAC) inhibitors. *Bioorg. Med. Chem. Lett. 16*, 4068−4070.
(45) Oka, N., and Greenberg, M. (2005) The effect of the 2-amino group of 7,8-dihydro-8-oxo-2′-deoxyguanosine on translesion synthesis and duplex stability. *Nucleic Acids Res. 33*, 1637−1643.
(46) Bodepudi, V., Shibutani, S., and Johnson, F. (1992) Synthesis of 2′-deoxy-7,8-dihydro-8-oxoguanosine and 2′-deoxy-7,8-dihydro-8-oxoadenosine and their incorporation into oligomeric DNA. *Chem. Res. Toxicol. 5*, 608−617.
(47) Porello, S., Williams, S., Kuhn, H., Michaels, M., and David, S. (1996) Specific recognition of substrate analogs by the DNA mismatch repair enzyme MutY. *J. Am. Chem. Soc. 118*, 10684−10692.
(48) Chepanoske, C., Porello, S., Fujiwara, T., Sugiyama, H., and David, S. (1999) Substrate recognition by Escherichia coli MutY using substrate analogs. *Nucleic Acids Res. 27*, 3197−3204.

DOI: 10.1021/acschembio.7b00389
ACS Chem. Biol. 2017, 12, 2335−2344